

New axisymmetric equilibria with flow from an expansion about the generalized Solovév solution

A. I. Kuiroukidis^{1*}, D. A. Kaltsas^{1†} and G. N. Throumoulopoulos^{1‡}

¹Department of Physics, University of Ioannina, GR 451 10 Ioannina, Greece

Emails: *a.kuirouk@uoi.gr, †kaltsas.d.a@gmail.com, ‡gthroum@uoi.gr

Abstract

We construct analytic solutions to the generalized Grad-Shafranov (GS) equation, adopting the general linearizing ansatz for the free-function terms it contains, by expanding the generalized Solovév solution [Ch. Simintzis, G. N. Throumoulopoulos, G. Pantis and H. Tasso, *Phys. Plasmas* **8**, 2641 (2001)]. On the basis of these solutions, we examine how the generalized Solovév configuration is modified as the values of the free parameters associated with the additional pressure, poloidal-current and electric-field terms are changed. Thus, a variety of equilibria of tokamak, spherical tokamak and spheromak pertinence are constructed including D-shaped configurations with positive and negative triangularity and diverted configurations with either a couple of X-points or a single X-point.

1 Introduction

The magnetohydrodynamics axisymmetric equilibrium states are governed by the well-known GS equation, a quasi-linear elliptic partial differential equation for the poloidal magnetic flux-function, containing a couple of arbitrary functions of that flux (surface functions), namely the pressure and the poloidal-current functions. This equation is generally solved numerically under appropriate boundary conditions, and to this end, several codes have been developed, e.g. the HELENA code [1]. Also, to easier gain physical intuition and for benchmarking equilibrium codes, analytic solutions have been constructed to linearized forms of the GS equation. In connection with the present study we first mention the widely employed in plasma confinement studies Solovév solution [2]. This solution, corresponding to constant surface-function terms in the GS equation, describes an up-down symmetric equilibrium with D-shaped magnetic surfaces surrounded by a spontaneously formed separatrix with a couple of X-points (cf. Fig. 1). Also, known is the Maschke-Hernegger solution [3, 4], expressed in terms of the Whittaker functions, corresponding to linear choices of the surface-function terms and describing more realistic equilibria with current-density profiles vanishing on the plasma boundary. Several additional analytic solutions to the GS equation are available, e.g. extending the Solovév solution by polynomial contributions to the homogeneous counterpart of the GS equation in order to construct diverted tokamak equilibria [5]; for constant pressure and linear current-density choices of the free terms in the GS equation [6]; for linear choices of both the pressure and current-density terms by imposing D-shaped boundaries or boundaries with a lower X-point [7, 8, 9]; by differentiation of known separated solutions with respect to the separation parameter in order to get simpler solutions [10]; and in elliptic prolate geometry [11]. Also, for the case of the generic linearized form of the GS equation an analytic solution

involving infinite series was derived in [12] and was employed to construct equilibrium configurations pertinent to the tokamak ASDEX-Upgrade.

Extended equilibrium investigations have been conducted to include plasma flows and associated electric fields, which play an important role in the creation of advanced confinement regimes in tokamaks, e.g. the transition of the low to high confinement mode. In particular, for incompressible flows, the generalized GS equation (1) shown below was derived [13, 14], containing five free surface quantities. Equation (1) has an additional electric-field term through the electrostatic potential Φ , associated with the component of plasma velocity non-parallel to the magnetic field. For parallel velocity and arbitrary assignment of the free surface-function terms, an extension of the HELENA code was developed in [15], while the generalized Solovév solution to (1) (given by (5) below), which constitutes a basic ingredient of the present study, was obtained in [14]. Owing to the electric field, the respective equilibrium in addition to a separatrix, similar to that of the usual static Solovév equilibrium, possess a third X-point outside the separatrix (cf. Fig. 11 of [14]). Other analytic solutions to the generalized GS equation of tokamak or space plasma pertinence were obtained by adopting a Solovév-like linearizing ansatz and imposing a diverted boundary [16]; alternative linearizing ansatzes [17, 18, 19]; non-linear forms of the generalized GS equation [20]; employing Lie-point symmetries for linear and nonlinear choices of the free-function terms [21, 22, 23]; and by the method of similarity reduction [24, 25].

Aim of the present work is to construct analytically solutions to the generalized GS equation in its generic linearized form by employing an alternative method. This consists in pursuing solutions as expanded generalized Solovév ones, i.e. as superposition of the generalized Solovév solution and a function to be determined. In addition to the novelty of this method we are particularly interested in examining how the Solovév configuration is modified when the influence of the expanding function becomes stronger by changing the pertinent new free parameters.

In section 2 the generalized GS equation and the generalized Solovév solution are briefly reviewed and the method of solving the generalized GS equation adopting the generic linearized ansatz is presented. Then, analytic solutions to the generic linearized generalized GS equation are constructed in section 3. In section 4 we examine how the Solovév configuration is modified by varying the additional free parameters associated with the pressure and the poloidal current in conjunction with the parallel component of the velocity and electric field, thus obtaining a variety of new configurations. The conclusions are summarized in section 5.

2 Generic linear axisymmetric equilibria with non-parallel flow

The generalized GS equation is given in SI units by (cf. [13, 14])

$$\Delta^* u + \frac{1}{2} \frac{d}{du} \left[\frac{X^2}{1 - M_p^2} \right] + \mu_0 R^2 \frac{dP_s}{du} + \mu_0 \frac{R^4}{2} \frac{d}{du} \left[\rho \left(\frac{d\Phi}{du} \right)^2 \right] = 0. \quad (1)$$

Here (R, ϕ, z) are cylindrical coordinate with z corresponding to the axis of symmetry; the poloidal magnetic flux function $u(R, z)$ labels the magnetic surfaces; $M_p(u)$ is the Mach function of the poloidal velocity with respect to the poloidal Alfvén velocity;

$\Phi(u)$ is the electrostatic potential; $\rho(u)$ is the plasma density; $X(u)$ relates to the toroidal magnetic field $B_\phi = I/R$ through

$$I = \frac{X}{(1 - M_p)} - R^2 \frac{\sqrt{\rho} M_p \Phi'}{(1 - M_p)^{1/2}}. \quad (2)$$

The operator Δ^* in (1) is $\Delta^* := \partial^2/\partial R^2 - (1/R)\partial/\partial R + \partial^2/\partial z^2$ and μ_0 is the permeability of free space. For vanishing flow, i.e. $M_p = \Phi' = 0$, the surface function $P_s(u)$ coincides with the pressure and Eq. (1) reduces to the GS equation.

Following Ref. [14] we make the following choice of the free surface-function terms in (1)

$$\begin{aligned} \frac{d(\mu_0 P_s)}{du} &= -\frac{P_{s0}}{U_0}, \\ \frac{1}{2} \frac{d}{du} \left[\frac{\mu_0 X^2}{1 - M_p^2} \right] &= \epsilon \frac{P_{s0} R_0^2}{U_0 (1 + \delta^2)}, \\ \frac{1}{2} \frac{d}{du} \left[\mu_0 \rho \left(\frac{d\Phi}{du} \right)^2 \right] &= -\lambda \frac{P_{s0}}{U_0 (1 + \delta^2) R_0^2}. \end{aligned} \quad (3)$$

Normalizing as $x := R/R_0$, $y := z/R_0$, $U := u/u_0$, $u_0 := P_{s0} R_0^4 / (2U_0 (1 + \delta^2))$, Eq. (1) assumes the form

$$U_{xx} - \frac{1}{x} U_x + U_{yy} - 2\epsilon x^4 + -2(1 + \delta^2)x^2 + 2\epsilon = 0, \quad (4)$$

and the generalized Solovév solution is given by

$$U_{gs} = \left[y^2 (x^2 - \epsilon) + \frac{\delta^2 + \lambda}{4} (x^2 - 1)^2 + \frac{\lambda}{12} (x^2 - 1)^3 \right]. \quad (5)$$

The equilibrium configuration for $\lambda > 0$ is shown in Fig. 1. As already mentioned in the Introduction, the outermost closed surface (red-dashed line) is a separatrix consisting of an elliptic outer part and a straight inner part parallel to the axis of symmetry; thus, a couple of X-points are created. Expressions of the X-point coordinates and of the inner and outer points of the configuration on the mid-plane $y = 0$ in terms of the parameters δ , ϵ and λ are given in the caption of Fig. 1. The magnetic axis is located at $(x = 1, y = 0)$. The parameter ϵ determines the compactness of the configuration, i.e. for $\epsilon > 0$ the equilibrium is diamagnetic and describes either a tokamak or a spherical tokamak, while for $\epsilon = 0$ the inner part of the separatrix touches the axis of symmetry forming a spheromak. The parameter δ relates to the elongation of the magnetic surfaces in the vicinity of the magnetic axis, i.e. the higher the value of δ , the larger the elongation parallel to the axis of symmetry. For $\lambda = 0$ the velocity becomes parallel to the magnetic field, while for $\lambda < 0$ a third X-point appears outside the separatrix. When the velocity vanishes ($M_p = \lambda = 0$), the usual static Solovév solution is recovered. Here we will consider equilibria with $\lambda > 0$.

We now try the following new generic linearizing ansatz to Eq. (1)

$$\begin{aligned} \frac{d(\mu_0 P_s)}{du} &= -\frac{P_{s0}}{U_0} + \bar{\alpha} \frac{P_{s0}}{U_0^2} u, \\ \frac{1}{2} \frac{d}{du} \left[\frac{\mu_0 X^2}{1 - M_p^2} \right] &= \epsilon \frac{P_{s0} R_0^2}{U_0 (1 + \delta^2)} - \bar{\beta} \epsilon \frac{P_{s0} R_0^2}{U_0^2 (1 + \delta^2)} u, \end{aligned}$$

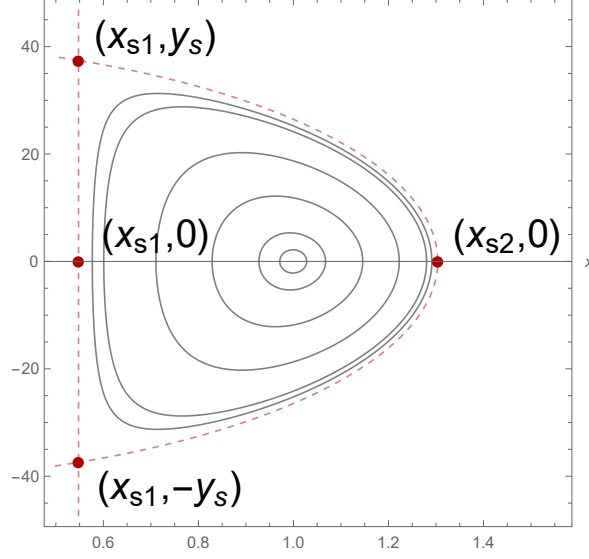


Figure 1: The equilibrium configuration of the GS solution (5). The red-dashed curve represents the separatrix with $x_{s1} = \sqrt{\epsilon}$, $x_{s2} = \left(-\epsilon\lambda - 3\delta^2 + \sqrt{3}\sqrt{-\epsilon^2\lambda^2 - 2\delta^2\epsilon\lambda + 3\delta^4 + \delta^2\lambda + 4\lambda^2}/(2\lambda)\right)^{1/2}$ and $y_s = [(1 - \epsilon)^2(2\delta^2 + \lambda(\epsilon + 1))]^{1/2}$.

$$\frac{1}{2} \frac{d}{du} \left[\mu_0 \rho \left(\frac{d\Phi}{du} \right)^2 \right] = -\lambda \frac{P_{s0}}{U_0(1 + \delta^2)R_0^2} + \bar{\gamma} \frac{\lambda P_{s0}}{U_0^2(1 + \delta^2)R_0^2} u, \quad (6)$$

where $\bar{\alpha}, \bar{\beta}, \bar{\gamma}$ are dimensionless parameters. Setting $G := 2\epsilon$, $F := -2(1 + \delta^2)$, $E := -2\lambda$, $\alpha := \bar{\alpha}(u_0/U_0)$, $\beta := \bar{\beta}(u_0/U_0)$ and $\gamma := \bar{\gamma}(u_0/U_0)$ we obtain from (1) the following equation:

$$U_{xx} - \frac{1}{x}U_x + U_{yy} + Ex^4 + Fx^2 + G - Ex^4\gamma U - Fx^2\alpha U - G\beta U = 0. \quad (7)$$

Note that the solution to (7) for $\alpha = \beta = \gamma = 0$ is given by (5). We now expand about the GS solution (5) as

$$U = U_{gs} + W(x, y), \quad (8)$$

with the function $W(x, y)$ to be determined so that (8) to satisfy (7). Substituting (8) into (7) yields

$$\begin{aligned} W_{xx} - \frac{1}{x}W_x + W_{yy} - \gamma Ex^4 W - \alpha Fx^2 W - \beta GW &= \\ &= (\gamma Ex^4 + \alpha Fx^2 + \beta G)U_{gs}. \end{aligned} \quad (9)$$

This is an inhomogeneous linear second-order partial differential equation for the unknown function $W(x, y)$. The general solution consists of the sum of the general solution to the counterpart homogeneous equation plus a particular solution of the complete inhomogeneous equation.

3 Solutions

We first consider the homogeneous counterpart of (9):

$$W_{xx} - \frac{1}{x}W_x + W_{yy} - (\gamma E x^4 + \alpha F x^2 + \beta G)W = 0. \quad (10)$$

The general solution of (10) can be found by separation of variables, i.e. in the form

$$W(x, y) = X(x)Y(y). \quad (11)$$

Inserting (11) into (10) we find:

$$Y'' + k^2 Y = 0, \quad (12)$$

and

$$X'' - \frac{1}{x}X' - (\gamma E x^4 + \alpha F x^2 + \beta G + k^2)X = 0, \quad (13)$$

where k is the parameter of separation. The general solution of (12) is

$$Y(y) = D_1 \cos(ky) + D_2 \sin(ky). \quad (14)$$

Setting $\xi = x^2$, Eq. (13) takes the form

$$4\xi X''(\xi) - (\gamma E \xi^2 + \alpha F \xi + \beta G + k^2)X = 0. \quad (15)$$

Since $\xi = 0$ is a regular singular point of (15) its solution can be derived by the method of Frobenius in terms of infinite converging series of the form:

$$X(\xi) = \sum_{n=0}^{\infty} a_n \xi^{n+r}. \quad (16)$$

Substituting (16) into (15) results in the following recursion relations:

$$\begin{aligned} 4r(r-1)a_0 &= 0, \\ 4r(r+1)a_1 - (\beta G + k^2)a_0 &= 0, \\ 4(r+1)(r+2)a_2 - \alpha F a_0 - (\beta G + k^2)a_1 &= 0, \\ (n \geq 2) \quad 4(n+r)(n+r+1)a_{n+1} - \gamma E a_{n-2} - \alpha F a_{n-1} - (\beta G + k^2)a_n &= 0, \end{aligned} \quad (17)$$

where a_0 is a freely specified parameter. The roots of the indicial polynomial, $r(r-1)$, are $r_1 = 1$ and $r_2 = 0$. Therefore, for $r_1 = 1$, one solution of (15) is

$$X_1(\xi) = \xi \sum_{n=0}^{\infty} a_n \xi^n. \quad (18)$$

Since $r_1 - r_2$ is a non-zero integer, the second linearly independent solution is of the form

$$X_2(\xi) = cX_1(\xi) \ln \xi + \sum_{n=0}^{\infty} \bar{a}_n \xi^n, \quad (19)$$

where the coefficients c and \bar{a}_n can be determined by substituting (19) into (15). Here, we will employ the solution $X_1(\xi)$.

Furthermore, we will pursue a particular solution of (9) in the form:

$$W(x, y) = W_1(x)y^2 + W_2(x). \quad (20)$$

Inserting (20) into (9) yields

$$W_1'' - \frac{1}{x}W_1' - (\gamma Ex^4 + \alpha Fx^2 + \beta G)W_1 = \left(x^2 - \frac{G}{2}\right)(\gamma Ex^4 + \alpha Fx^2 + \beta G), \quad (21)$$

and

$$\begin{aligned} & W_2'' - \frac{1}{x}W_2' + 2W_1 - (\gamma Ex^4 + \alpha Fx^2 + \beta G)W_2 = \\ & = - \left[\frac{(F + E + 2)}{8}(x^2 - 1)^2 + \frac{E}{24}(x^2 - 1)^3 \right] (\gamma Ex^4 + \alpha Fx^2 + \beta G). \end{aligned} \quad (22)$$

Equation (21) involves only the function $W_1(x, y)$. Thus, once (21) is solved, the solution contributes to the inhomogeneous part of (22).

To solve (21) we again change variable, $\xi = x^2$, to get:

$$4\xi W_1''(\xi) - (\gamma E\xi^2 + \alpha F\xi + \beta G)W_1 = \left(\xi - \frac{G}{2}\right)(\gamma E\xi^2 + \alpha F\xi + \beta G). \quad (23)$$

Setting

$$W_1 + \left(\xi - \frac{G}{2}\right) := \bar{W}_1, \quad (24)$$

Eq. (23) is put in the form:

$$4\xi \bar{W}_1'' - (\gamma E\xi^2 + \alpha F\xi + \beta G)\bar{W}_1 = 0. \quad (25)$$

For $\beta = 0$, the solution of (25) is:

$$\bar{W}_1 = c_1 Ai\left(\frac{\alpha F + \gamma E\xi}{(2\gamma E)^{2/3}}\right) + c_2 Bi\left(\frac{\alpha F + \gamma E\xi}{(2\gamma E)^{2/3}}\right), \quad (26)$$

where Ai and Bi are the Airy functions of the first and second kind. For $\beta \neq 0$ apart from the k^2 -term, Eq. (15) is identical with (25). Therefore a solution of (25) is:

$$\bar{W}_1(\xi) = \xi \sum_{n=0}^{\infty} d_n \xi^n, \quad (27)$$

with the coefficients d_n being determined by the recurrence relations (17) after setting $k = 0$ (and replacing a_n with d_n).

Lastly, we will obtain a particular solution of the inhomogeneous equation (22). Introducing once more the variable $\xi = x^2$, Eq. (22) is written as:

$$\begin{aligned} & 4\xi W_2''(\xi) - (\gamma E\xi^2 + \alpha F\xi + \beta G)W_2 = \\ & = -2W_1(\xi) - [C_5\xi^5 + C_4\xi^4 + C_3\xi^3 + C_2\xi^2 + C_1\xi + C_0], \end{aligned} \quad (28)$$

where $W_1 = \bar{W}_1 - (\xi - G/2)$ by (24) and

$$\begin{aligned}
C_5 &= \gamma \frac{E^2}{24}, \\
C_4 &= \frac{\gamma E(F+2)}{8} + \alpha F \frac{E}{24}, \\
C_3 &= \beta G \frac{E}{24} + \alpha F \frac{(F+2)}{8} - \gamma E \frac{(2F+E+4)}{8}, \\
C_2 &= \beta G \frac{(F+2)}{8} - \alpha F \frac{(2F+E+4)}{8} + \gamma E \frac{(3F+2E+6)}{24}, \\
C_1 &= -\beta G \frac{(2F+E+4)}{8} + \alpha F \frac{(3F+2E+6)}{24}, \\
C_0 &= \beta G \frac{(3F+2E+6)}{24}.
\end{aligned} \tag{29}$$

In view of the converging series solutions (18) and (27) to the respective homogeneous equations (15) and (25), we pursue a similar in form solution to (28):

$$W_2 = \xi \sum_{n=0}^{\infty} b_n \xi^n. \tag{30}$$

Inserting (30) into (28) we obtain after some tedious but straightforward algebra that b_0 is freely specified and

$$\begin{aligned}
C_0 + G &= 0, \\
8b_1 - \beta G b_0 + 2d_0 - 2 + C_1 &= 0, \\
24b_2 - \alpha F b_0 - \beta G b_1 + 2d_1 + C_2 &= 0, \\
48b_3 - \gamma E b_0 - \alpha F b_1 - \beta G b_2 + 2d_2 + C_3 &= 0, \\
80b_4 - \gamma E b_1 - \alpha F b_2 - \beta G b_3 + 2d_3 + C_4 &= 0, \\
120b_5 - \gamma E b_2 - \alpha F b_3 - \beta G b_4 + 2d_4 + C_5 &= 0, \\
(n \geq 6) \quad 4n(n+1)b_n - \gamma E b_{n-3} - \alpha F b_{n-2} - \beta G b_{n-1} + 2d_{n-1} &= 0.
\end{aligned} \tag{31}$$

Inspection of the last of Eqs. (29) and $C_0 + G = 0$ (first of Eqs. (31)) together with the definitions $G := 2\epsilon$, $F := -2(1 + \delta^2)$ and $E := -2\lambda$ implies the following:

1. When $\beta = 0$, then $\epsilon = 0$ and therefore the second of (6) becomes $(1/2)d/du(X^2/(1 - M_p^2)) = 0$. In the absence of flow then (2) implies that the plasma is confined by a vacuum toroidal magnetic field ($\beta_p = 1$ equilibrium); when the non-parallel flow is there the electric-field term in (2) additionally contributes to the poloidal current.
2. When $\epsilon \neq 0$ and $\beta \neq 0$, the last of (29) becomes $\beta(3F + 2E + 6) + 24 = 0$. In this case all the linear terms in the ansatz (6) can remain finite. The latter relation just acts as a constraint on the parameters ϵ , δ and λ . To construct the equilibria of Sec. 4 we treated ϵ and λ as free and

$$\delta = \left[\frac{(2/3)(6 - \beta\lambda)}{\beta} \right]^{1/2}. \tag{32}$$

3. When $\epsilon = 0$, β does not necessarily vanish and both δ and λ remain free.

Additional free parameters are α , β , γ , a_0 , d_0 , b_0 , D_1 , D_2 , R_0 , P_{s0} , U_0 and k . Also, it is noted that the series expansion (30) was shown numerically to converge and we kept terms up to the order of ξ^{20} in our calculations.

Summarizing, a solution of the general linearized form of the generalized GS equation (9) consists of a separated solution of its homogeneous counterpart in terms of (11), (14) and (18) plus a particular solution of the form (20), expressed in terms of the series (27) and (30).

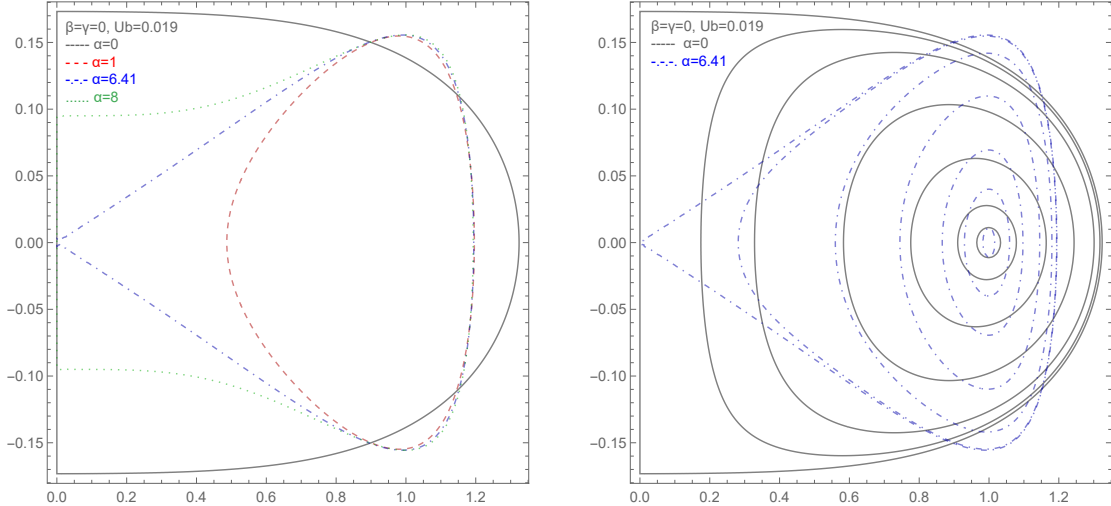


Figure 2: Left: different equilibrium boundaries are given as the additional linear-in- U , pressure term in the first of (6) varies in connection with different values of α . The black continuous curve represents the separatrix of the respective generalized Solovév spheromak configuration. Right: a set of magnetic surfaces for one of the configuration represented by blue, dot-dashed U -curves are shown together with the respective curves of the generalized Solovév equilibrium.

4 Equilibrium configurations

By employing the solution to (7) derived in the previous section we have constructed several new equilibria. Particularly, we examined how the generalized Solovév equilibrium is modified by varying the additional parameters α , β and γ , associated with the respective linear-in- u terms in (6) of pressure, poloidal-current in conjunction with the poloidal velocity, and electric field. To impose a stagnation point, (x_0, y_0) , in addition to the conditions $dU/dx|_{x_0, y_0}$ and $dU/dy|_{x_0, y_0}$ we considered the sign of the quantity

$$\left. \frac{d^2U}{dx^2} \frac{d^2U}{dy^2} - \left(\frac{d^2U}{dxdy} \right)^2 \right|_{(x_0, y_0)},$$

which should be positive for a magnetic axis and negative for an X-point. For the up-down symmetric configurations considered, the magnetic axis is located at the same position, $(x = 1, y = 0)$ as the generalized Solovév configuration and $U = U_a = 0$ thereon. Note that in this case the condition $dU/dy|_{(1,0)}$ is identically satisfied because of symmetry. If not otherwise specified, we assigned the following parametric values:

$k = 0.1$, $\delta = 0.1$, $\lambda = 0.1$, $D_1 = 1$ and $D_2 = 0$. It is recalled that when $\beta \neq 0$ and $\epsilon \neq 0$, δ should be calculated from (32). The parameters a_0 , b_0 and d_0 were determined as solutions to the set of the algebraic equations derived by the conditions associated with the imposition of a stagnation point. Since we employed dimensionless quantities, the reference dimensional parameters R_0 , P_{s0} (in units of $4\pi \times 10^{-7} \text{ H/m Pa}$) and U_0 remained free. Depending on the value of ϵ we constructed tokamak, spherical tokamak and spheromak equilibria, the latter corresponding to $\epsilon = 0$.

First, we examined the impact of the α - β - and γ -term individually on up-down symmetric equilibria equilibria by imposing the same position of the magnetic axis, $(x = 1, y = 0)$, as that of the respective generalized Solovév equilibrium and the same value $U = 0$ thereon. In the presence of α -term, a D-shaped configuration is formed with negative triangularity, the boundary of which is shown in Fig. 2-left by the red-dashed curve. As α gradually takes larger values the configuration increasing triangularity extends towards the axis of symmetry, touches the axis of symmetry forming a separatrix with a single X-point located on the origin of the coordinate system (blue, dot-dashed line) and then becomes a peculiar configuration having a separatrix with a couple of X-points (green-dotted line).

The β -term creates configurations with small triangularity elongated along the x -axis as shown in Fig. 3. The red-dashed curves represent the magnetic surfaces of a configuration with the same poloidal magnetic flux as the respective generalized Solovév tokamak configuration represented by the black-continuous curve. As β takes larger values the configuration gets more extended and eventually reaches the axis of symmetry becoming a spheromak one. It is noted that for $\epsilon = \beta = \gamma = 0$ the equilibrium becomes independent of β . The impact of the γ -term is similar to that of the α -term as shown in Fig. 4.

Subsequently, the impact of combinations of the α -, β - and γ -terms was examined by imposing an X-point at several positions. Thus, a variety of configurations were created. Three examples are given in Figs. 5-7. In Fig. 5 the blue, dot-dashed curves represent an up-down symmetric spherical tokamak configuration ($\epsilon = 0.1$) the X-points of which are common with those of the respective generalized Solovév equilibrium, but the poloidal magnetic flux of this former equilibrium is larger than that of the latter. The red-dashed curve represents the boundary of a D-shaped configuration with poloidal magnetic flux equal to that of the generalized Solovév solution. In Fig. 6 is shown an up-down symmetric diverted configuration with the imposed X-points located at $(x = 0.84, y = \pm 14.5)$, while Fig. 7 shows an up-down asymmetric configuration with the magnetic axis located at $(x = 1.02, y = 0.83)$ and the single lower X-point at $(x = 0.94, y = -22.6)$.

5 Conclusions

Making a generic linearizing choice of the free function-terms involved in the generalized GS equation (1) we solved the resulting linearized equation (9) analytically. The requested solution was expressed as an expansion of the generalized Solovév solution (5) in the form (8) involving the determinable function W . Then, the solution was obtained as a superposition of the counterpart homogeneous equation and a particular solution of the complete inhomogeneous equation in the form (20). The solutions of the pertinent radial ODEs were expressed in terms of infinite converging series.

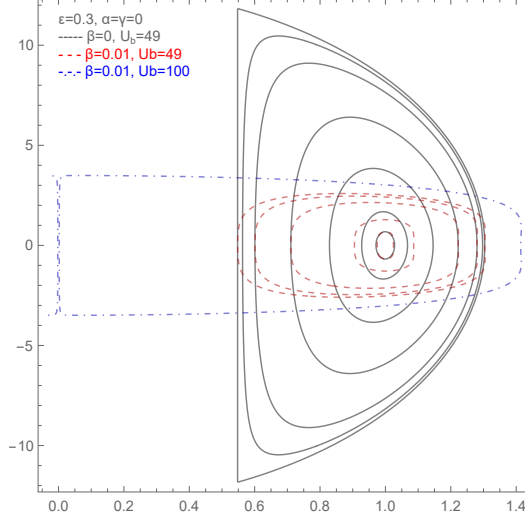


Figure 3: The impact of the additional linear-in- U , poloidal-current term in the second of (6) in connection with different values of β . The black continuous curves represent the magnetic surfaces of the respective generalized Solovév tokamak configuration.

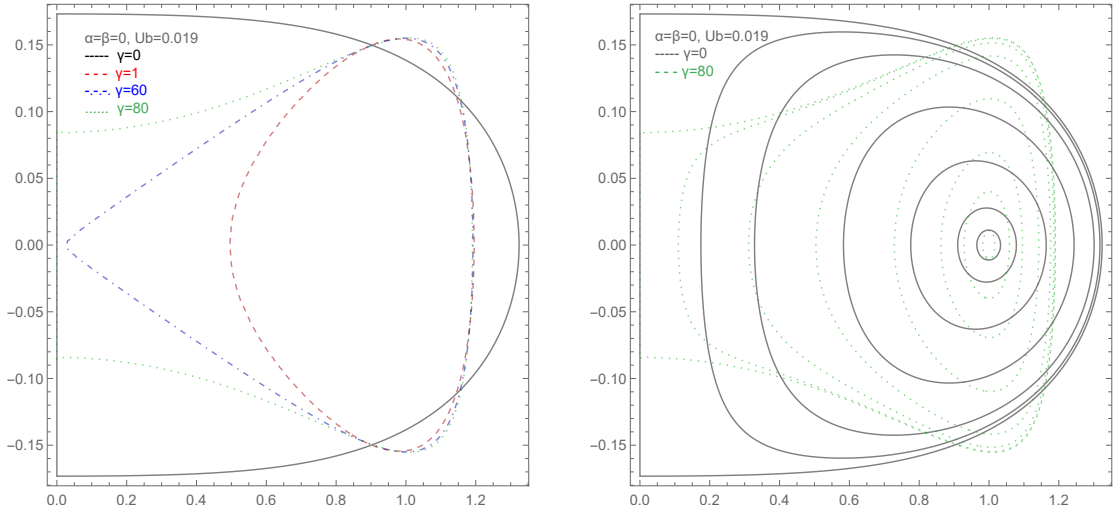


Figure 4: Left: different equilibrium boundaries are given as the additional linear-in- U , electric-field term in the third of (6) varies in connection with different values of γ . The black continuous curve represents the separatrix of the respective generalized Solovév spheromak configuration. Right: A set of magnetic surfaces for one of the configuration represented by green-dotted U-curves are shown together with the respective curves of the Solovév equilibrium.

Employing these solutions, we constructed several configurations by changing the values of the free parameters, either individually or in combination, associated with the new terms of pressure, poloidal current and electric field. The equilibria constructed are pertinent to tokamaks, spherical tokamaks and spheromaks; they include D-shaped configurations with either positive or negative triangularity and diverted configurations with either a couple of X-points or a single X-point.

The present study can be extended to a more generic generalized GS equation

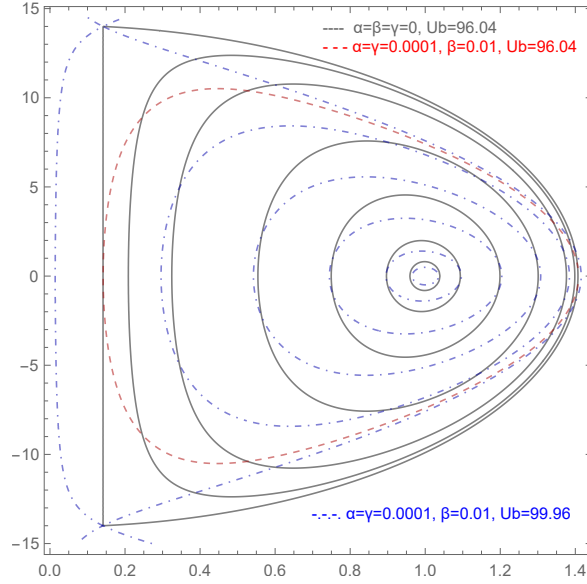


Figure 5: A spherical tokamak diverted configuration ($\epsilon = 0.1$, $\delta = 20$) with a couple of X-points common with the respective Solovév equilibrium. The red-dashed curve represents the boundary of a D-shaped tokamak equilibrium with poloidal magnetic flux equal to that of the Solovév one.

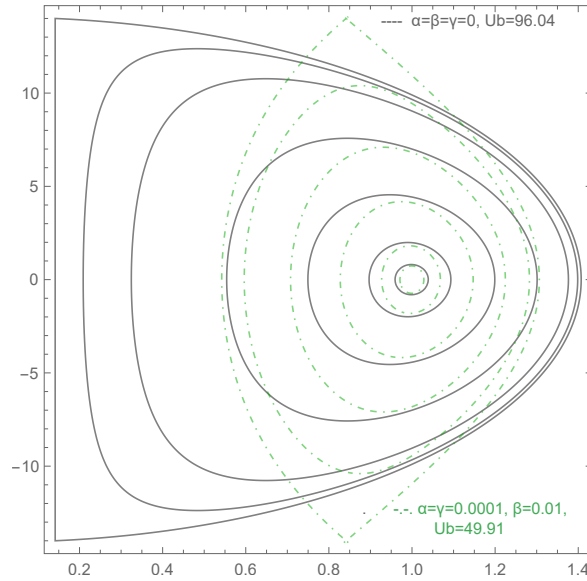


Figure 6: An up-down symmetric, diverted tokamak configuration ($\epsilon = 0.1$, $\delta = 20$) with a couple of X-points located at $(x = 0.84, y = \pm 14.5)$. The black continuous curves represent the magnetic surfaces of the respective Solovév equilibrium.

accounting for CGL pressure anisotropy ([26], Eq. (34) therein). Another extension could be pursued in the framework of Hall-MHD, a simplified two-fluid model with inertialess electron-fluid elements keeping on magnetic surfaces and ion-fluid elements departing from them.

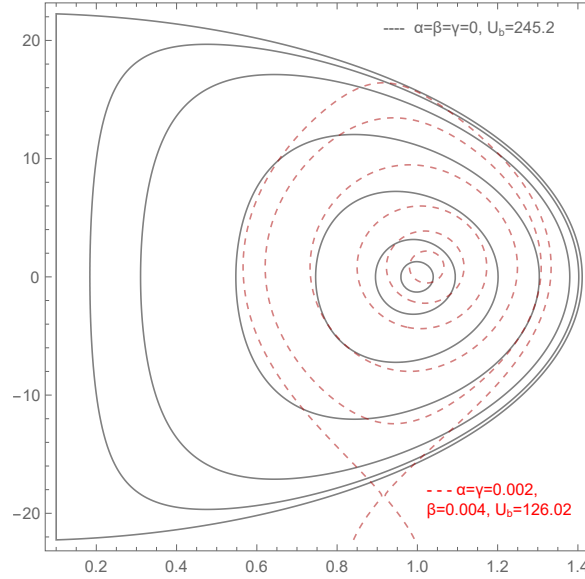


Figure 7: An up-down asymmetric, diverted tokamak configuration for $k = 0.2$, $\epsilon = 0.2$, $\delta = 31.6$, $D_1 = 0.5$ and $D_2 = 0.01$. The magnetic axis is located at $(x = 1.02, y = 0.83)$ and the single lower X-point at $(x = 0.94, y = -22.6)$. The black continuous curves represent the magnetic surfaces of the respective Solovév equilibrium.

Acknowledgments

This work was conducted in the framework of participation of the University of Ioannina in the National Programme for the Controlled Thermonuclear Fusion, Hellenic Republic.

References

- [1] C. Konz, W. Zwingmann, F. Osmanlic, B. Guillerminet, F. Imbeaux, P. Huynh, M. Plociennik, M. Owsiak, T. Zok, and M. Dunne, “*First physics applications of the Integrated Tokamak Modelling (ITM-TF) tools to the MHD stability analysis of experimental data and ITER scenarios,*” in EPS (2011), p. 2. <https://info.fusion.ciemat.es/OCS/EPS2011ABS/pdf/02.103>
- [2] L. S. Solovév, JETP **26**, 400 (1968). http://www.jetp.ras.ru/cgi-bin/dn/e_026_02_0400
- [3] F. Herrnegger, “*On the equilibrium and stability of the belt pinch*”, Proceedings of V. European Conference on Controlled Fusion and Plasma Physics, Grenoble, August 1972, Vol. I, p. 26 (1972).
- [4] E. K. Maschke, Plasma Phys. **15**, 535 (1973). <https://dx.doi.org/10.1088/0032-1028/15/6/006>
- [5] R. Srinivasan, L. L. Lao and M. S. Chu, Plasma Phys. Control. Fusion **52**, 035007 (2010). <https://dx.doi.org/10.1088/0741-3335/52/3/035007>

- [6] E. Mazzucato, Phys. Fluids **18**, 536 (1975). <https://doi.org/10.1063/1.861186>
- [7] L. Guazzotto and J. P. Freidberg, Phys. Plasmas **14**, 112508 (2007). <https://doi.org/10.1063/1.2803759>
- [8] Antoine J. Cerfon and Jeffrey P. Freidberg, Phys. Plasmas **17**, 032502 (2010). <https://doi.org/10.1063/1.3328818>
- [9] Antoine J. Cerfon and Michael O’Neil, Phys. Plasmas **21**, 064501 (2014). <https://doi.org/10.1063/1.4881466>
- [10] D. Pfirsch, E. Rebhan, Nucl. Fusion **14**, 547 (1974). <https://dx.doi.org/10.1088/0029-5515/14/4/011>
- [11] F. Crisanti, J. Plasma Phys. **85**, 905850210 (2019). <https://doi.org/10.1017/S0022377819000175>
- [12] C. V. Atanasiu, S. Günter and K. Lackner, I.G.Miron, Phys. Plasmas, **11**, 3510 (2004). <https://doi.org/10.1063/1.1756167>
- [13] H. Tasso and G. N. Throumoulopoulos, Phys. Plasmas, **5**, 2378 (1998). <https://doi.org/10.1063/1.872912>
- [14] Ch. Simintzis, G. N. Throumoulopoulos, G. Pantis, H. Tasso, Phys. Plasmas **8**, 2641 (2001). <https://doi.org/10.1063/1.1371768>
- [15] G. Poulipoulis, G. N. Throumoulopoulos, C. Konz, and ITM-TF Contributors, Phys. Plasmas **23**, 072507 (2016). <https://doi.org/10.1063/1.4955326>
- [16] D. A. Kaltsas and G. N. Throumoulopoulos, Phys. Plasmas **21**, 084502 (2014). <https://doi.org/10.1063/1.4892380>
- [17] Bingren Shi, Nucl. Fusion **51**, 023004 (2011). <https://dx.doi.org/10.1088/0029-5515/51/2/023004>
- [18] Ap. Kuiroukidis and G. N. Throumoulopoulos, Phys. Plasmas **23**, 114502 (2016). <https://doi.org/10.1063/1.4967346>
- [19] D. A. Kaltsas, A. Kuiroukidis and G. N. Throumoulopoulos, Phys. Plasmas **26**, 124501 (2019). <https://doi.org/10.1063/1.5120341>
- [20] Salah Moawad, Zeitschrift für Naturforschung A **73**, 371 (2018). <https://doi.org/10.1515/zna-2017-0309>
- [21] Ap. Kuiroukidis and G. N. Throumoulopoulos, Phys. Plasmas **23**, 112508 (2016). <https://doi.org/10.1063/1.4968235>
- [22] Ap. Kuiroukidis and G. N. Throumoulopoulos, Phys. Plasmas **21**, 032509 (2014). <https://doi.org/10.1063/1.4869248>
- [23] G. Poulipoulis, G. N. Throumoulopoulos, Phys. Plasmas **30**, 114501 (2023). <https://doi.org/10.1063/5.0174091>

- [24] D. A. Kaltsas and G. N. Throumoulopoulos, Phys. Lett. A **380**, 3373 (2016). <https://doi.org/10.1016/j.physleta.2016.08.011>
- [25] A. I. Kuiroukidis, D. A. Kaltsas, G. N. Throumoulopoulos, Phys. Plasmas **31**, 042503 (2024). <https://doi.org/10.1063/5.0198558>
- [26] A. Evangelias, G. N. Throumoulopoulos, Plasma Phys. Control. Fusion **58**, 045022 (2016). <https://dx.doi.org/10.1088/0741-3335/58/4/045022>